Equilibrium fractionation and isotope exchange kinetics between aqueous Se(IV) and Se(VI)

Decan Tan [a,c], Jian-Ming Zhu [b,*], Xiangli Wang [d,e,*], Thomas M. Johnson [f]
Shehong Li [a], Wenpo Xu [a,c]

[a] *State Key Laboratory of Environmental Geochemistry, Institute of Geochemistry, Chinese Academy of Sciences, Guiyang 550081, China*
[b] *State Key Laboratory of Geological Processes and Mineral Resources, China University of Geosciences, Beijing 100083, China*
[c] *University of Chinese Academy of Sciences, Beijing 100049, China*
[d] *Department of Marine Sciences, University of South Alabama, Mobile, AL 36688, USA*
[e] *Dauphin Island Sea Lab, Dauphin Island, AL 36528, USA*
[f] *University of Illinois at Urbana-Champaign, Department of Geology, 1301 W Green Street, Urbana, IL 61801, United States*

Abstract

The selenium (Se) isotope system has been proposed as a redox proxy in environmental and paleoceanographic studies. However, Se isotope exchange among various Se species can potentially interfere with redox-related isotope signatures, and is still poorly understood. In this work, we investigated Se isotope exchange kinetics and equilibrium fractionations between aqueous Se(IV) and Se(VI) under various experimental conditions. At pH = 7, low-Se concentration experiments (0.026 mM Se(IV) and 0.026 mM Se(VI)) at 25 °C, 38 °C and 60 °C were conducted for 900 days, while high-Se concentrations (0.13 mM Se (IV) and 0.14 mM Se(VI); 1.3 mM Se(IV) and 1.4 mM Se(VI)) at 60 °C were conducted for 1547 days. All experiments did not reach isotopic equilibrium, with observed Se isotope fractionations <0.20‰. Adding an electronic shuttle (Anthraquinone-2, 6-disulfonate) did not increase the isotope exchange rate. These results show that under the experimental conditions examined, the isotope exchange reaction between aqueous Se(IV) and Se(VI) is extremely slow.

The exchange kinetics between Se(IV) and Se(VI) were also investigated using a ^{82}Se tracer. The exchange rates (R) at 0.13 mM Se(IV) and 0.13 mM Se(VI) at 25 °C, 38 °C and 60 °C were determined to be $\leq 6.34 \times 10^{-10}$ M day^{-1}, $\leq 1.12 \times 10^{-09}$ M day^{-1} and $\leq 1.17 \times 10^{-09}$ M day^{-1}, respectively. Using the upper bound for the isotope exchange rate at 25 °C and theoretically calculated equilibrium fractionations, and assuming a first order isotope exchange reaction between Se(IV) and Se(VI) by analogy to the sulfur system, the timescale of isotope exchange between aqueous Se (IV) and Se (VI) in a natural lake (Sweitzer Lake, Colorado, USA) was estimated. The minimum half-time (t$_{1/2}$, time to reach 50% isotopic equilibrium) and the minimum time for detectable isotope exchange (t$_{min}$) are $\geq$440,000 and $\geq$18,000 years, respectively. In the modern oceans, t$_{1/2}$ and t$_{min}$ are $\geq$51 million and $\geq$3.6 million years, respectively. These timescales are much longer than the residence time of Se in Sweizer Lake (2.4 years) and the modern ocean (26,000 years). Therefore, when using Se isotopes to trace the biogeochemical cycle of Se in lakes and oceans, the effect caused by isotope exchange between aqueous Se(IV) -Se (VI) systems is insignificant.

---

* Corresponding authors at: China University of Geosciences (Beijing), Beijing 100083, China (J.-M. Zhu); Department of Marine Sciences, University of South Alabama, Mobile, AL 36688, USA (X. Wang).
E-mail addresses: jmzhu@cugb.edu.cn (J.-M. Zhu), xwang@southalabama.edu (X. Wang).

1. INTRODUCTION

Selenium is a redox sensitive element with four main valences in nature: -II (Se^{2-}, HSe^-, and organic Se), 0 (Se0), IV (SeO_3^{2-}, $HSeO_3^-$, and H_2SeO_3) and VI (SeO_4^{2-}, $HSeO_4^-$ and H_2SeO_4) (Robberecht and Grieken, 1982; Cutter, 1982; Brookins, 1988; Johnson, 2004; Zhu et al., 2004). Se(IV) and Se(VI) are the dominant species in oxic environments (McNeal and Balistrieri, 1989; Johnson et al., 2000; Herbel et al., 2002; Clark and Johnson, 2010; Qin et al., 2017a, 2017b). However, in reducing environments, Se oxyanions (Se(IV) + Se(VI)) can be reduced to elemental Se and the metal selenides (Oremland et al., 1989; Frankanberger and Benson, 1994; Shaker, 1996; Zhu et al., 2004, 2012; Clark and Johnson, 2010). Elemental Se and selenides are almost insoluble in water and thus Se is nearly immobile in reducing environments. In contrast, Se oxyanions are soluble and mobile, and they can be adsorbed to iron-manganese oxides and organic matter (Balistrieri and Chao, 1990; Zhang and Sparks, 1990; Saeki and Matsumoto, 1994; Saeki et al., 1995; Pezzarossa et al., 1999; Catalano et al., 2006; Duc et al., 2003, 2006; Rovira et al., 2008). Since Se(IV) is more easily adsorbed than Se(VI) (Balistrieri and Chao, 1990; Duc et al., 2006; Mitchell et al., 2013), a large proportion of Se(IV) is absorbed onto sediments, which makes Se (VI) predominating in lakes and oceans. The ratio of Se (IV)/ Se (VI) is generally less than 1 in rivers and surface seawater (Measures and Burton, 1980; Measures et al., 1984; Cutter and Bruland, 1984; Aono et al., 1991; Cutter and Cutter, 1995, 1998, 2001, 2004; Hung and Shy, 1995; Yao and Zhang, 2005; Chang, 2017).

Selenium has six stable isotopes: ^{74}Se (0.89%), ^{76}Se (9.37%), ^{77}Se (7.64%), ^{78}Se (23.77%), ^{80}Se (49.61%) and ^{82}Se (8.73%). The study of Se isotope fractionation can be dated back to 1962, when Krouse and Thode (1962) first measured Se isotope fractionations ($\delta^{82/76}Se_{reactant}$ - $\delta^{82/76}Se_{product} = 15‰$) during reduction of Se(VI) to Se(0) using NH_2OH at room temperature. Johnson (2004) systematically summarized Se isotope fractionation induced by oxidation, reduction, adsorption, methylation and biological assimilation. The reviewed studies found Se isotope fractionations caused by abiotic and/or biotic reduction of Se (VI) to Se(IV) and Se(IV) to Se(0) to be 3.90–11.04‰ and 8.25–12.6‰ (relative to NIST SRM 3149), respectively (Johnson et al., 1999; Johnson and Bullen, 2003; Herbel et al., 2000; Ellis et al., 2003), and by oxidation of elemental Se and Se(IV) to Se(VI) to be less than 1‰ (Johnson et al., 1999; Schilling et al., 2015). The fractionation of Se isotopes during adsorption processes is relatively small, generally less than 1‰ (Johnson et al., 1999; Mitchell et al., 2013). The $\triangle^{82/76}Se$ ($\delta^{82/76}Se_{solution}$-$\delta^{82/76}Se_{solid}$) of Se(IV) adsorbed onto iron oxide is less than 1.0‰, while $\triangle^{82/76}Se$ for the Se(VI) adsorbed onto iron oxide is less than 0.2‰ (Mitchell et al., 2013; Xu et al., 2020). Selenium isotope fractionation in assimilation and methylation for Se oxyanions by algae, phytoplankton and large plants is small ($\triangle^{82/76}Se < 1.5‰$) (Johnson et al., 2000; Herbel et al., 2002;

Clark and Johnson, 2010), but it is larger (<4.5‰) during the methylation and volatilization processes by fungi (Schilling et al., 2011, 2013).

The selenium isotope system has been applied to tracing the biogeochemical transformations of Se in various environmental settings (Johnson et al., 1999, 2000; Herbel et al., 2002; Rouxel et al., 2004; Clark and Johnson, 2010; Layton-Matthews et al., 2013; Zhu et al., 2014; Schilling et al., 2015), to reconstructing the redox conditions of the atmosphere-ocean system over various spatial and temporal scales (Mitchell et al., 2012, 2016; Wen et al., 2014; Pogge von Strandmann et al., 2015; Stüeken et al., 2015a,b,c; Stüeken, 2017; Kipp et al., 2017; König et al., 2019), and to investigating the origin and evolution of Earth's volatiles (Labidi et al., 2018; Yierpan et al., 2018, 2019; Varas-Reus et al., 2019). However, as one of the fundamental prerequisites for understanding the application of Se isotopes, isotope exchange between different valence states of Se has received little attention. Studies on isotope exchange for other elements such as Cr, U, Mg and Fe has found significant equilibrium isotope fractionations (Wang et al., 2015a,b; Zink et al., 2010; Johnson et al., 2002; Welch et al., 2003; Skulan et al., 2002; Wiesli et al., 2004; Beard et al., 2010; Wu et al., 2010, 2011; Gorski et al., 2012; Frierdich et al., 2014a, 2014b; Reddy et al., 2015; Li et al., 2011, 2015; Shahar et al., 2008; Macris et al., 2013). Meanwhile, in the past 60 years, equilibrium isotope exchange and kinetic effects between different speciation of sulfur have been extensively studied and applied (Mcdonald, 1961; Igumnov, 1976; Sakai and Dickson, 1978; Sakai, 1983; Fossing et al., 1992; Eldridge et al., 2016). However, studies on equilibrium isotope fractionation between different Se speciation have been limited to theoretical calculations (Krouse and Thode, 1962; Schauble, 2004; Li and Liu, 2011).

Selenium (IV) and Se(VI) are the two most predominant species in the surface environment, and they can coexist for a long time. For example, the residence times of Se in one lake was reported to 2.4 years (Clark and Johnson, 2010) whereas in the ocean it was estimated at 26,000 years (Large et al., 2015). First-principles calculations showed that equilibrium Se isotope fractionation between Se(IV) and Se(VI) at 25 °C is 13.78‰ (for $HSeO_3^-$- SeO_4^{2-}) or 13.28‰ (for SeO_3^{2-}- SeO_4^{2-}) (Li and Liu, 2011), but the timescales for detectable isotope exchange are unknown. Therefore, experimental determination of the equilibrium fractionation and isotope exchange kinetics between Se (IV) and Se (VI) are of great significance to the application of Se isotope system to tracking geochemical processes. In this work, we investigated Se isotope exchange kinetics between $HSeO_3^-$ and SeO_4^{2-} at pH = 7 under different experimental temperatures and at different Se concentrations. An electronic shuttle (Anthraquinone-2, 6-disulfonate, AQDS) was also tested for its capability of promoting electron transfer between Se(VI) and Se(IV) and thus enhancing isotope exchange rates. A ^{82}Se tracer was used in some of the experiments to increase the ability to detect slow isotope exchange.

2. EXPERIMENTS AND METHODS

2.1. Materials and reagents

Na_2SeO_3 and Na_2SeO_4 powders (>98.0% purity) and an ^{82}Se spike solution were purchased from Alfa Aesar. 80 mg Na_2SeO_3 and 180 mg Na_2SeO_4 powders were used to prepare 5.98 mM Se(IV) and 13 mM Se(VI) solutions, with their $\delta^{82/76}Se$ measured to be $-1.18 \pm 0.10‰$ (2SD, n = 8) and $-0.60 \pm 0.10‰$ (2SD, n = 8), respectively. Before the experiment, the pH of Se(IV) and Se(VI) stock solution was adjusted to 7 with a buffer (25 mM HEPES) and stored at 4 °C. A solution of Se(IV) enriched in ^{82}Se ($\delta^{82/76}Se = 1089 \pm 8‰$ (2SD, n = 22)) was prepared by mixing 0.65 mM ^{82}Se and 0.65 mM Na_2SeO_3 solution at a ratio of 1:1. Sodium hydroxide (pellets, 98% purity), 1.0 N Sodium hydroxide (Acculute Standard Volumetric Solution), trace metal HNO_3 and analytical grade HCl were obtained from Thermo Fisher Scientific. The ultrapure water used in this work was purified by a Milli-Q Element system (Millipore, USA). The AG1-X8 anion resin (200–400 mesh, Bio-Rad) was cleaned in turn with methanol, 1 M NaOH, 1 M HCl and stored in 0.1 M HCl.

2.2. Experimental design

2.2.1. Isotope exchange experiments of aqueous Se(IV)-Se(VI)

Isotope exchange rate is influenced by the reactant concentration and temperature (Johnson et al., 2002; Welch et al., 2003; Wang et al., 2015a,b). Therefore, we conducted our experiments at different temperatures and Se concentrations. High-Se and high-T experiments were designed to obtain the equilibrium fractionation factor in a reasonable duration of time, while low-Se and low-T experiments were designed to measure isotope exchange kinetics in conditions closer to natural environments.

Low-Se experiments with 0.026 mM Se(IV) and 0.026 mM Se(VI) were conducted at 25 °C (EXP 1), 38 °C (EXP 2) and 60 °C (EXP 3). High-Se experiments were all conducted at 60 °C, with 0.13 mM Se(IV) and 0.14 mM Se(VI) for EXP 4, and 1.3 mM Se(IV) and 1.4 mM Se(VI) for EXP 5. In order to promote isotope exchange, an electron shuttle, 0.2 M 2,6-anthraquinone disulphonate (AQDS), was added to two experiments at 25 °C (EXP 6) and 60 °C (EXP 7), both with 1.3 mM Se(IV) and 1.9 mM Se(VI). Quinones are the dominant redox active moieties associated with natural organic matter (Nurmi and Tratnyek, 2002). AQDS, which has a quinone moiety, is a widely used model electron shuttle to represent natural organic matter. The advantage of using AQDS is that there has been good understanding of this molecule. To demonstrate that the HEPES buffer does not interfere with isotope exchange. We conducted one control experiment without HEPS buffer at pH 3.5 and 60 °C with 0.13 mM Se(IV) and 0.13 mM Se(VI).

All experiments used 10 mM NaCl solution as the background electrolyte to keep the ionic strength the same for all experiments, and were buffered at pH 7 by 25 mM HEPES buffer. Se(IV) and Se(VI) solutions with a total volume of 20 mL were mixed in a 30 ml serum bottle. Pure N_2 was used to purge the solution for 20 min to remove oxygen. The sealed experimental vessels were placed in a thermostat oscillator at 25 °C and two thermostat water baths at 38 ± 2 °C and 60 ± 2 °C, respectively. At each sampling time point, 0.2 mL sample solution was withdrawn from the bottle, and the volume was replenished with N_2. After the sample was taken out, it was immediately diluted to 200 ng/mL with ultra-pure water and processed through anion exchange columns to separate Se(IV) and Se(VI).

2.2.2. Kinetic isotope exchange experiment

Given slow isotope exchange rates based on the experiments mentioned above, we used an ^{82}Se-enriched Se(IV) in order to detect small extent of isotope exchange, following a similar experimental scheme in Welch et al. (2003) and Wang et al. (2015a). Briefly, 0.65 mM Se (IV) with a $\delta^{82/76}Se$ of $1089 \pm 8‰$ (2SD, n = 22) and 0.65 mM Na_2SeO_4 with a $\delta^{82/76}Se$ of $-0.60 \pm 0.10‰$ (2SD, n = 8) were mixed at 1:1 mass ratio. This solution was then diluted to 0.13 mM Se(IV) and 0.13 mM Se(VI), injected into three 30 mL serum bottles each containing 10 mL solution, and sealed after 20 min nitrogen purging. These bottles were placed on thermostat oscillator maintained at 25 °C (EXP 8), 38 °C (EXP 9) and 60 °C (EXP 10). Subsequent steps were the same as those described in Section 2.2.1.

2.3. Separation of Se(IV) and Se(VI)

The procedures for separating aqueous Se(IV) and Se(VI) were modified from Ellis et al. (2003) and Clark and Johnson (2010), which took advantage of Se(IV) and Se(VI) having different affinities with an anion exchange resin (AG1-X8, 200–400 mesh) when they are dissolved in HCl of different concentrations. We tested the method and obtained the elution curve that clearly shows good separation of Se(IV) and Se(VI) from sample solution (Fig. S1). The recoveries for Se(IV) and Se(VI) were nearly 100% (Table 1). The separated $\delta^{82/76}Se(IV)$ and $\delta^{82/76}Se(VI)$ values were consistent with the isotopic composition of stock-Se(IV) and stock-Se(VI) (Table 1). Briefly, 1 mL of AG1-X8 resin was filled into 10 mL Bio-Rad Polyprep columns. The resin was cleaned with 10 mL 6 M HCl and rinsed with MQ water until the eluent became neutral, and then conditioned with MQ water. Sample solutions were diluted with MQ water to 200 ng/mL Se(IV) and 200 ng/mL Se(VI), and then taking 1 mL of diluted solutions were loaded onto the columns. Matrix elements were rinsed off the columns by 5 mL MQ water. After that, Se(IV) and Se(VI) were eluted with 5 mL 0.1 M HCl and 5 mL 5 M HCl, respectively. In order to minimize cross-contamination between ^{82}Se-enriched Se(IV) and isotopically natural Se(VI), the elution volume for Se(IV) was increased from 5 mL to 8 mL for the ^{82}Se-enriched experiments.

2.4. Se concentration and isotope measurement

The concentrations of Na_2SeO_3, Na_2SeO_4, ^{82}Se tracer, and separated Se(IV) and Se(VI) were determined by

Table 1
Cross-contamination during ion exchange separation of Se (IV) and Se (VI).

Sample number	Recovery (%) for Se(IV)	Recovery (%) for Se(VI)	$\delta^{82/76}$Se(IV), ‰	$\delta^{82/76}$Se(VI)[#], ‰	$\delta^{82/76}$Se(VI)[*], ‰
Stock-Se			**−1.18**	**−0.60**	
Test 1	99.82	99.76	−1.18	−0.58	−0.58
Test 2	98.14	99.58	−1.20	−0.65	−0.65
Test 3	99.12	102.99	−1.20	−0.53	−0.53
Test 4	100.94	100.74	−1.12	−0.62	−0.62
Test 5	99.61	100.63	−1.22	−0.64	−0.64
Test 6	98.51	102.66	−1.31	−0.72	−0.72
Average	**99.36**	**101.02**	**−1.21**	**−0.62**	**−0.62**
2SD	**2.01**	**2.93**	**0.13**	**0.13**	**0.13**
Stock-Se			**1089**	**−0.60**	
Test 7	98.13	100.31	1091	5.01	−0.45
Test 8	101.08	99.86	1098	1.99	−3.52
Test 9	99.85	100.20	1087	1.94	−3.51
Test 10	100.45	99.53	1090	4.83	−0.63
Test 11	98.62	101.74	1089	7.94	2.50
Test 12	98.43	102.57	1088	5.58	0.14
Test 13	98.49	103.32	1087	3.14	−2.19
Average	**99.29**	**101.08**	**1090**	**4.35**	**−1.11**
2SD	**2.15**	**2.94**	**7.66**	**4.31**	**4.34**

[#] No cross-contamination correction.
[*] Corrected for cross-contamination.

hydride generation atomic fluorescence spectrometry (HG-AFS) at the Institute of Geochemistry, Chinese Academy of Sciences. 0.2% NaOH-1.5% KBH_4 (w/w) was used as a reductant to convert Se(IV) to H_2Se (Zhu et al., 2008, 2014). For Se(VI) samples, Se(VI) was first reduced to Se (IV) by 5 M HCl before being analyzed. The concentrations of separated Se(IV) and Se(VI) were also obtained by the double spike technique (see below), and used to monitor whether there was reduction or oxidation occurring during the experiments.

The $\delta^{82/76}$Se values were determined on the Nu Plasma II MC-ICPMS (Nu instrument, UK) at the State Key Laboratory of Environmental Geochemistry, Institute of Geochemistry, Chinese Academy of Sciences. The mass discrimination effect of the instrument and potential isotope fractionation during sample preparation processes were corrected by a ^{74}Se-^{77}Se double spike (DS) technique (Zhu et al., 2008, 2014). Since the recoveries of Se(IV) and Se(VI) were ~100%, no detectable isotope fractionation occurs in this purification process. Therefore, the DS can be added after column separation. We confirmed this by processing NIST 3149 (Se(IV) + Se(VI)) through the same procedures, which yielded a value of 0.03 ± 0.06‰ (2SD, n = 3) for separated Se(IV) and 0.01 ± 0.07‰ (2SD, n = 3) for separated Se(VI) (Table S1). In addition, the newly mixed solution in EXP 1–10 was separated, and the isotopic composition of Se (IV) and Se (VI) after separation was consistent with stock-Se(IV) and stock-Se(VI) (Table 1). Therefore, the ^{74}Se-^{77}Se DS in the form of Se(IV) was added after column separation but the separated Se (VI) was firstly mixed with DS and then reduced by 5 M HCl. A ^{77}Se$_{spike}$/^{78}Se$_{sample}$ ratio of 2 was aimed to minimize errors during data reduction. Sample-spike mixtures were allowed to equilibrate overnight before measurement on the instrument. These operations ensured

that the addition of double spike after Se(IV)-Se(VI) separation is acceptable.

The Nu plasma II MC-ICPMS is equipped with 16 Faraday cups: Ax, L5, L2, H2, H6 and H8 were used to receive signals of ^{76}Se, ^{74}Se, ^{77}Se, ^{78}Se, ^{80}Se and ^{82}Se, respectively; L4, IC2 and H7 were used to monitor the interferences of ^{75}As, ^{73}Ge and ^{81}Br, respectively. The samples were introduced into the plasma through a hydride generation system that converts Se (IV) to H_2Se (Rouxel et al., 2002; Zhu et al., 2008). The instrument was operated in the low resolution mode. With an injection concentration of ~6 ng/mL and an injection rate of 0.7 mL/min, the signal intensity of ^{82}Se was commonly ~1.5–2 V. The polyatomic interferences of $^{36}Ar^{40}Ar^+$, $^{38}Ar^{40}$-Ar^+ on ^{76}Se and ^{78}Se were subtracted through On Peak Zero (OPZ) measurements and a secondary correction derived from measurement of the combined signal from ^{80}Se and ^{40}-$Ar^{40}Ar^+$ at m/z = 80 (Zhu et al., 2008). Correction for interferences of Ge^+, AsH^+ and BrH^+ was similar to that of Clark and Johnson (2010). Each measurement consisted of 3 blocks, with each blocking comprising 10 cycles and each cycle lasting 5 seconds. One NIST 3149 standard solution was measured every 3–5 samples to monitor instrument drift, which was typically <0.10‰ within a year. Analytical accuracy was monitored by measuring the laboratory standard MH495 ($\delta^{82/76}$Se = −3.44 ± 0.10‰) and GBW-Se ($\delta^{82/76}$Se = −7.92 ± 0.10‰) every 10 samples. Here, the uncertainty of $\delta^{82/76}$Se values in all experiments were estimated by measuring the isotope composition of separated Se (IV) and Se (VI) from a mixed Se (IV)-Se (VI) solution. Analytical uncertainty for both $\delta^{82/76}$Se (IV) and $\delta^{82/76}$Se (VI) in experiments without ^{82}Se-tracer were ±0.13‰ (2SD, n = 6) (Table 1), while for the experiments with ^{82}Se-tracer used, the uncertainty were ±7.66‰ (2SD, n = 7) for $\delta^{82/76}$Se (IV) and ±4.34‰ (2SD, n = 7) for $\delta^{82/76}$Se (VI) (Table 1).

2.5. Correction for cross-contamination during the separation of Se(IV) and Se(VI)

Although there is small cross-contamination between Se (VI) and Se(IV) during column separation, because only Se (IV) was reduced by KBH$_4$, the concentration and isotopic composition of Se(IV) was not affected by the contamination from Se(VI). On the other hand, Se(VI) needs to be reduced to Se (IV) before hydrogenation. Therefore, cross contamination of Se(IV) on Se(VI) will jeopardize the determined concentration and isotopic composition of Se(VI). The kinetic experiments were particularly prone to cross-contamination because the $\delta^{82/76}$Se(IV) value was very large (1089 ± 8‰). For instance, if 5% Se(IV) enters into Se(VI), it can cause a deviation of ~50‰ in measured $\delta^{82/76}$Se(VI).

Four separation experiments were conducted to test the separation efficiency with AG1-X8 resin. Tests 1–6 were duplicate experiments with 200 ng/mL Se (IV) mixed with 200 ng/mL Se (VI), both with normal isotopic compositions ($\delta^{82/76}$Se(IV) = −1.18 ± 0.10‰ (2SD, n = 8) and $\delta^{82/76}$Se (VI) = −0.60 ± 0.10‰ (2SD, n = 8)); Test 7–13 are duplicate experiments with 200 ng/mL ^{82}Se-enriched Se (IV) ($\delta^{82/76}$Se(IV) = 1089. ± 8‰; 2SD, n = 22) and 200 ng/mL normal Se(VI) ($\delta^{82/76}$Se(VI) = −0.60 ± 0.10‰;2SD, n = 8). The results are shown in Table 1. The recoveries of Se(IV) and Se(VI) in Test 1–6 were 99.36 ± 2.01% (2SD, n = 6) and 101.02 ± 2.93% (2SD, n = 6), respectively. Measured $\delta^{82/76}$Se(IV) was −1.21 ± 0.13‰ (2SD, n = 6) and $\delta^{82/76}$Se(VI) was −0.62 ± 0.13‰ (2SD, n = 6), both in agreement with those of unprocessed mother solutions. For Test 7–13, the recoveries of Se (IV) and Se (VI) were 99.29 ± 2.17% (2SD, n = 7) and 101.08 ± 2.94% (2SD, n = 7), respectively. The $\delta^{82/76}$Se(VI) = 4.35 ± 4.31‰ (2SD, n = 7) was slightly heavier than that of

Table 2

Se isotope shifts driven by Se (IV) - Se (VI) exchange without an electronic shuttle.

Time (days)	[Se(IV)]/[Se(VI)][a]	$\delta^{82/76}$Se(IV) ‰	$\delta^{82/76}$Se(VI) ‰	$\delta^{82/76}$Se(VI) * ‰	Offset VI-IV* ‰	F Se(IV)	F Se(VI)
EXP 1: Temperature:25°C; pH = 7; 0.026 mM Se(IV)-0.026 mM Se(VI)							
0	1.02	**−1.20**	**−0.60**	**−0.62**	**0.60**		
2	1.05	−1.21	−0.53	−0.53	0.69	0.002	0.011
6	1.09	−1.18	−0.65	−0.65	0.53	−0.003	−0.007
30	1.03	−1.23	−0.66	−0.66	0.57	0.005	−0.009
85	1.00	−1.22	−0.51	−0.51	0.71	0.003	0.014
214	1.02	−1.15	−0.58	−0.58	0.57	−0.008	0.004
456	1.03	−1.24	−0.56	−0.56	0.68	0.006	0.007
907	1.08	−1.22	−0.62	−0.62	0.60	0.003	−0.003
EXP 2: Temperature:38°C; pH = 7; 0.026 mM Se(IV)-0.026 mM Se(VI)							
2	1.03	−1.11	−0.49	−0.49	0.62	−0.015	0.019
6	1.05	−1.23	−0.64	−0.64	0.59	0.005	−0.006
30	1.08	−1.22	−0.61	−0.61	0.61	0.003	−0.001
85	1.05	−1.18	−0.54	−0.54	0.64	−0.003	0.010
214	1.05	−1.25	−0.61	−0.61	0.64	0.008	−0.001
456	1.04	−1.12	−0.65	−0.65	0.47	−0.013	−0.008
907	1.04	−1.20	−0.71	−0.71	0.49	0.000	−0.018
EXP 3: Temperature:60°C; pH = 7; 0.026 mM Se(IV)-0.026 mM Se(VI)							
2	0.94	−1.11	−0.55	−0.55	0.56	−0.017	0.010
6	1.04	−1.22	−0.59	−0.59	0.63	0.004	0.002
30	1.05	−1.29	−0.78	−0.78	0.51	0.017	−0.033
214	1.06	−1.23	−0.56	−0.56	0.67	0.006	0.008
456	1.01	−1.20	−0.65	−0.65	0.55	0.000	−0.009
907	1.04	−1.35	−0.67	−0.67	0.68	0.028	−0.012
EXP 4: Temperature:60°C; pH = 7; 0.13 mM Se(IV)-0.14 mM Se(VI)							
2	0.92	−1.33	−0.65	−0.65	0.68	0.023	−0.009
5	0.94	−1.18	−0.64	−0.64	0.54	−0.004	−0.007
40	0.93	−1.16	−0.67	−0.67	0.49	−0.007	−0.013
577	0.88	−1.07	−0.43	−0.43	0.64	−0.023	0.033
847	0.86	−1.18	−0.59	−0.59	0.59	−0.004	0.003
1547	0.82	−1.15	−0.66	−0.66	0.49	−0.009	−0.011
EXP5:Temperature:60°C; pH = 7; 1.3 mM Se(IV)-1.4 mM Se(VI)							
2	0.95	−1.25	−0.67	−0.67	0.58	0.009	−0.013
5	0.92	−1.21	−0.66	−0.66	0.55	0.002	−0.011
160	0.93	−1.19	−0.63	−0.63	0.56	−0.002	−0.005
577	0.90	−1.17	−0.57	−0.57	0.60	−0.005	0.006
847	0.89	−1.13	−0.64	−0.64	0.49	−0.012	−0.007
1547	0.81	−1.22	−0.57	−0.57	0.66	0.005	0.006

[a] Concentration ratio of Se(IV) to Se(VI); F refer to Eq. (3).

* Corrected for cross contamination.

mother Se(VI) solution, due to cross-contamination by Se (IV).Therefore, the measured $\delta^{82/76}$Se(VI) in the kinetic experiment needs to be effectively corrected for cross-contamination.

The correction method for cross contamination between Se(IV) and Se(VI) was accomplished by solving simple mixing equations (Wang et al., 2015a,b):

$$\delta^{82/76}Se(VI)^* = \frac{\delta^{82/76}Se(VI) - f \cdot \delta^{82/76}Se(IV)}{1 - f} \qquad (1)$$

where f is the mass fraction of Se(IV) in the Se(VI) sample, $\delta^{82/76}$Se(IV) and $\delta^{82/76}$Se(VI) are the measured values of Se (IV) and Se(VI) after separation, respectively, and $\delta^{82/76}$Se (VI)* is the corrected value of Se(VI). The average recoveries of Se(IV) and Se(VI) were 99.32% (n = 13) and 101.05 % (n = 13), respectively (Test 1 through Test 13 in Table 1). However, since Se(IV) loss could also have occurred during sample loading and MQ rinsing, Se(IV) cross-over into Se (VI) would be <0.57% (i.e. $f < 0.0058$: 0.0058/(1.0105 + 0.0058)). In this paper, we assumed $f = 0.005$ to calculate cross contamination of Se(IV) on Se(VI). For EXP 1–7, the correction is smaller than the analytical precision for normal samples of ±0.2‰ (2SD) (Tables 2 and 3). However, for EXP 8–10, the correction is 5.31‰ on average (Table 4). Errors in estimating the recoveries of Se(IV) and Se(VI) could lead to errors in the correction. However, this level of error is smaller than the analytical precision for samples at ∼1100‰ levels, which was ±7.66‰ (Table 1).

3. RESULTS

The results for low-Se exchange experiments without AQDS are shown in Table 2 and Fig. 1A–C. After 900 days, all $\delta^{82/76}$Se values were, within analytical uncertainty, the same as the starting mother solutions. Similar results were observed for high-Se isotope exchange experiments without AQDS at 60 °C (Table 2 and Fig. 1D and E even after 1547 days of reaction. The values of $\triangle^{82/76}$Se$_{IV-IV}$ are 0.48‰ and 0.66‰, respectively, which are the same

as the 0.58‰ initial difference between $\delta^{82/76}$Se (VI) and $\delta^{82/76}$Se (IV). At high Se concentrations and temperatures, adding AQDS did not improve isotope exchange rates (Table 3, Fig. 2). The control experiment with no HEPES added at pH ∼7 and 3.5 also did not show detectable isotope exchange (Figs. S2, S3). For experiments EXP 8–10, utilizing the ^{82}Se tracer, there appeared to be some systematic increase in $\delta^{82/76}$Se(VI) after 910 days of exchange (Table 4, Fig. 3). However, the changes of $\delta^{82/76}$Se(IV) in EXP 8 (correlation coefficient r = 0.44, p = 0.38) and EXP 9 (r = 0.55, p = 0.26) were not statistically significant by Pearson correlation test at the level of 0.05. However, the $\delta^{82/76}$Se(IV) of EXP 10 had a significant positive relationship with time (r = 0.85, and p = 0.03), indicating that a small amount of isotopic exchange occurred.

4. DISCUSSION

4.1. Oxidation and reduction during isotope exchange

In these experiments, potential oxidation of Se(IV) or reduction of Se(VI) can lead to isotope fractionation (Rees and Thode, 1966; Johnson et al., 1999; Herbel et al., 2000; Johnson and Bullen, 2003; Ellis et al., 2003; Schilling et al., 2015) and interfere with the experiments' ability to determine the effects of isotope exchange. In this paper, we used the concentration ratio of Se(IV) to Se(VI) (i.e. [Se(IV)]/[Se(VI)]) to monitor whether oxidation of Se (IV) and/or reduction of Se(VI) occurred. In EXP 1–3 and EXP 8–10, the initial [Se(IV)]/[Se(VI)] was targeted to be 1.0, with an estimated range of 0.86–1.14 (1.00 ± 0.14, 2SD, n = 200; Monte- Carlo method for error calculation) based on a ±5% analytical error in Se concentration measurement by HG-AFS or MC-ICP-MS analysis. In EXP 4–5 and EXP 6–7, the range of [Se(IV)]/[Se(VI)] stay in the ranges of 0.78–1.02 and 0.60–0.80, respectively. Hence, the measured data (Table 2–4, Figs. 1–3) in all experiments show that the Se(IV)/Se(VI) remained unchanged within the analytical uncertainty.

Table 3
Se isotope shifts driven by Se (VI) - Se (VI) exchange with AQDS electronic shuttle.

Time (Days)	[Se(IV)]/[Se(VI)][a]	$\delta^{82/76}$Se(IV) ‰	$\delta^{82/76}$Se(VI) ‰	$\delta^{82/76}$Se(VI)* ‰	Offset IV-VI* ‰	F Se(IV)	F Se(VI)
EXP 6: Temperature:25°C; pH = 7; 1.3 mM Se(IV)-1.9 mM Se(VI), 0.2 M AQDS							
0	0.70	**−1.18**	**−0.60**	**−0.62**	**0.56**		
24	0.79	−1.38	−0.53	−0.53	0.85	0.023	0.014
65	0.68	−1.14	−0.69	−0.69	0.45	−0.008	−0.016
95	0.65	−1.23	−0.67	−0.67	0.56	0.004	−0.013
365	0.69	−1.16	−0.70	−0.70	0.46	−0.005	−0.018
425	0.74	−1.07	−0.67	−0.67	0.40	−0.017	−0.013
1095	0.64	−1.17	−0.63	−0.63	0.54	−0.004	−0.005
EXP 7: Temperature:60°C; pH = 7; 1.3 mM Se(IV)-1.9 mM Se(VI), 0.2 M AQDS							
24	0.76	−1.29	−0.45	−0.45	0.85	0.015	0.035
65	0.67	−1.13	−0.69	−0.69	0.44	−0.011	−0.020
95	0.78	−1.29	−0.63	−0.63	0.66	0.014	−0.006
365	0.73	−1.12	−0.73	−0.73	0.39	−0.012	−0.029
425	0.65	−1.28	−0.64	−0.64	0.64	0.012	−0.008
1095	0.74	−1.19	−0.61	−0.61	0.58	−0.002	−0.002

[a] Concentration ratio of Se(IV) to Se(VI).
* Correction for cross contamination.

Table 4
Results of kinetic isotope exchange experiments using ^{82}Se-enriched Se (IV).

Times, days	[Se(IV)]/[Se(VI)]	$\delta^{82/76}$Se (IV) ‰	$\delta^{82/76}$Se (VI) ‰	$\delta^{82/76}$Se(VI) * ‰	Offset IV-VI*‰	F Se(IV)	F Se(VI)	Recovery % Se(IV)	Recovery % Se(VI)
EXP 8: Temperature:25°C; pH = 7; 0.13 mM Se(IV) −0.13 mM Se(VI)									
(R ≤ 6.34 × 10^{-10} M day^{-1})									
0		**1089**	**−0.60**	**−1.11**	−1090				
28	1.03	1091	5.81	1.30	−1090	−0.004	0.003	99.41	98.13
78	1.06	1087	5.22	0.79	−1087	0.003	0.003	101.85	95.72
108	1.09	1089	7.07	2.34	−1087	−0.001	0.005	102.20	97.88
231	1.01	1087	8.79	3.36	−1084	0.003	0.007	98.84	98.21
820	0.97	1088	7.25	1.81	−1086	0.002	0.004	99.16	102.45
910	1.01	1090	8.67	3.24	−1087	−0.001	0.004	99.30	99.21
EXP 9: Temperature:38°C; pH = 7; 0.13 mM Se(IV) −0.13 mM Se(VI)									
(R ≤ 1.12 × 10^{-09} M day^{-1})									
28	0.99	1094	5.74	0.30	−1094	−0.010	0.002	98.59	104.09
78	1.02	1088	4.81	−0.64	−1089	0.001	0.000	99.11	98.96
108	1.02	1090	6.76	1.32	−1089	−0.003	0.003	99.55	98.28
231	0.99	1087	3.94	−1.51	−1088	0.007	−0.002	97.06	97.88
820	1.00	1088	5.44	0.01	−1088	0.002	0.001	99.60	97.41
910	1.04	1088	9.19	3.76	−1084	0.001	0.008	101.61	98.05
EXP 10: Temperature:60°C; pH = 7; 0.13 mM Se(IV) −0.13 mM Se(VI)									
R$^{\#}$ = 5.61 × 10^{-10}M day-1, (R ≤ 1.17 × 10^{-09} M day^{-1})									
28	0.96	1096	5.24	−0.21	−1096	−0.013	0.001	97.71	103.70
78	0.99	1088	5.04	−0.41	−1088	0.003	0.000	100.04	103.04
108	0.99	1089	6.25	0.81	−1088	0.000	0.003	99.03	101.55
231	0.90	1087	3.80	−1.65	−1088	0.004	−0.002	98.23	101.13
820	0.98	1088	7.83	2.40	−1086	0.000	0.005	100.42	100.81
910	0.95	1084	9.86	4.44	−1079	0.010	0.009	98.60	104.31

* Correction for Cross Contamination.
\# since measured values for EXP 10 has a clear statistical significance, here, the exact R value is given.
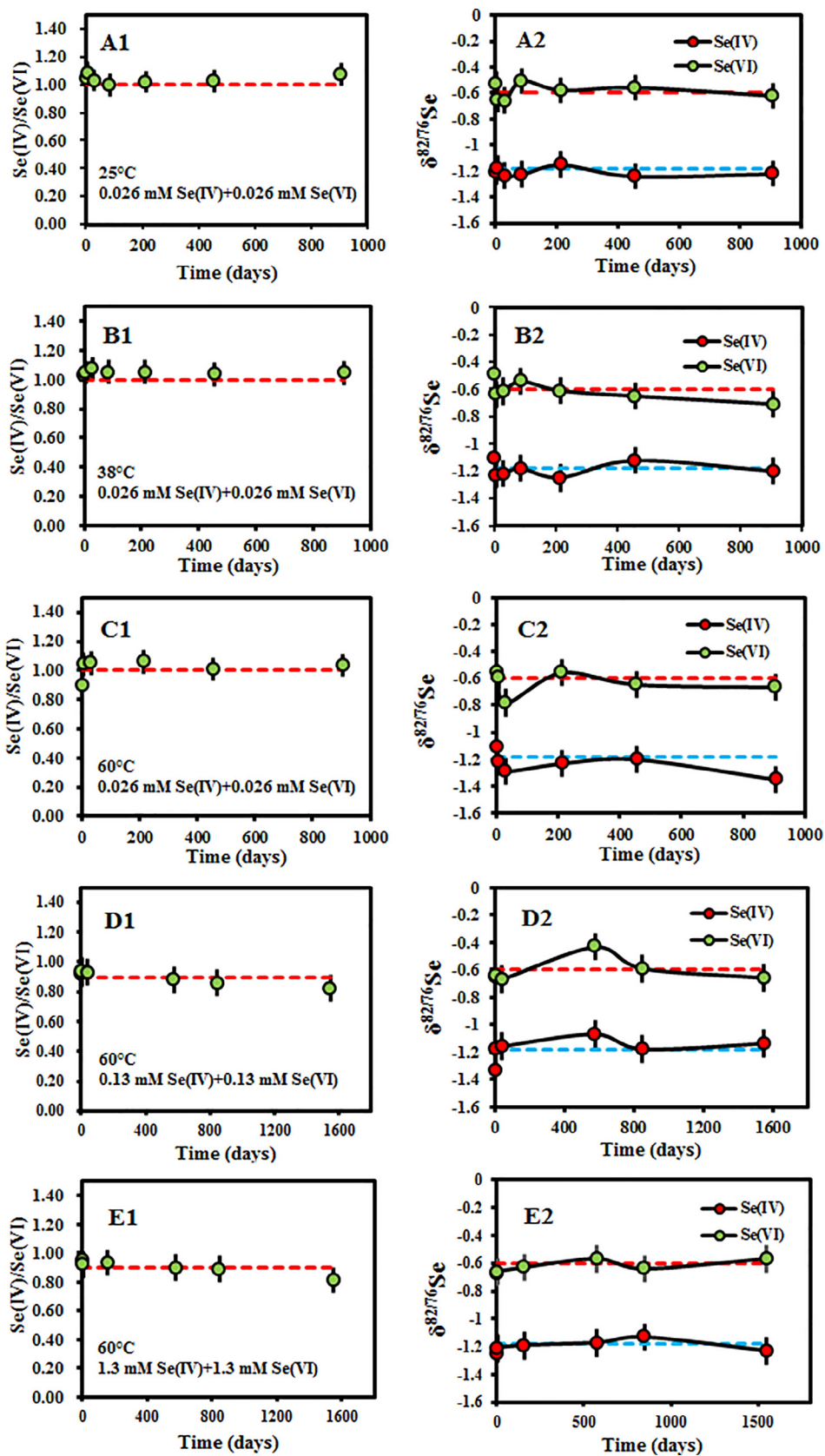
4.2. Effects of Se speciation on equilibrium isotope fractionation

At pH = 7 and 0.01 M ionic strength, $HSeO_3^-$ (94.5%) is the main Se(IV) species, with a small amount of SeO_3^{2-} (5.15%). In contrast, SeO_4^- (99.99%) is the dominant Se (VI) species, with negligible $HSeO_4^-$ (calculated using MINEQL 3.0; Table S2). Therefore, under the experimental conditions, the equilibrium fractionation between Se(IV) and Se(VI) should be controlled by isotope exchange between $HSeO_3^-$ and SeO_4^{2-}, and between SeO_3^{2-} and SeO_4^{2-}, with the latter pair generating an equilibrium fractionation 0.5‰ smaller than the former pair (Table S3; Li and Liu, 2011). Because this difference is small, the values of $\Delta^{82/76}Se_{VI-IV}$ caused by exchange reactions between $HSeO_3^-$ and SeO_4^{2-}, and SeO_3^{2-} and SeO_4^{2-} are considered approximately equal for the purposes of the calculations below.

4.3. Extraction of isotope exchange rates

Although most experiments in this study yielded constant $\delta^{82/76}Se(IV)$ and $\delta^{82/76}Se(VI)$ after 3 to 4 years of reaction, the $\delta^{82/76}Se(VI)$ values for EXP 8,9 and 10 seem to have increased (Table 4 and Fig. 3). According to Pearson correlation test, only EXP 10 showed statistically significant change (see Section 3), and thus can be used to calculate the isotope exchange rate at 60 °C. Although the $\delta^{82/76}Se(IV)$ in EXP 8 and 9 did not change significantly, we provided estimates for the upper bounds of possible rates of EXP 8 and 9. Here, we acknowledge that these calculated exchange rates are only first order approximations. Isotope exchange rate can be derived using the equation formulated by Mckay (1938):

$$-Ln(1-F) = R \cdot \frac{[Se(IV)] + [Se(VI)]}{[Se(IV)][Se(VI)]} \cdot t \qquad (2)$$

where t is the time in days; [Se(IV)] and [Se(VI)] are the concentrations of Se (IV) and Se (VI), respectively; R is the isotope exchange rate in M day^{-1}; F is the reaction extent, calculated by

$$F = \frac{\delta_t - \delta_i}{\delta_e - \delta_i} \qquad (3)$$

where δ refers to $\delta^{82/76}Se$, and i, t, and e represent "initial", "time", and "equilibrium", respectively (Mcdonald, 1961; Welch et al., 2003).

Since the equilibrium fractionation between Se(IV) and Se(VI) could not be determined even after more than 3 years of experiments, the previous three-isotope (Shahar et al., 2008; Cao and Bao, 2017) and multi-direction methods (Welch et al., 2003; Frierdich et al., 2014a) do not work well here. Hence, we used theoretically calculated equilibrium isotope fractionations between $HSeO_3^-$ and SeO_4^{2-}

(13.78‰, 12.83‰, 11.44‰ for 25 °C, 38 °C and 60 °C, respectively; Li and Liu, 2011). Using these fractionations, together with $\delta_i(IV)$ and $\delta_i(VI)$ values and mass ratio of Se (IV) and Se(VI), $\delta(IV)$ and $\delta_e(VI)$ can be calculated for EXP 1–7 (-7.80‰, −7.33‰, −6.63‰, −6.83‰, −6.83‰, −9.03‰ and −7.64‰ for Se(IV), and 5.98‰, 5.51‰, 4.81‰, 4.61‰, 4.61‰, 4.75‰ and 3.80‰ for Se(VI)). According to Eq. (3), F values for Experiments 1–3 at 900 days are all <0.03 (Table 2). Similarly, the F values For EXP 4–5 are also < 0.03 (Table 2).

Adding AQDS (EXP 6–7) did not lead to significant isotopic exchange. There are two possible reasons: (1) isotope exchange between Se(IV) and Se(VI) is extremely slow, and increased exchange rates caused by AQDS are still difficult to detect with the methods used in these experiments; (2) AQDS does not effectively change the electron transfer mechanism between Se(IV) and Se(VI). Future experiments are needed to investigate this further. The HEPES buffer used was an organic molecule that can potentially affect isotope exchange. However, the control experiment with no HEPES added did not show detectable isotope exchange after 847 days (Fig. S3).

Measurement of $\delta^{82/76}Se(IV)$ values at roughly 1089‰ is prone to large errors due to ordinary laboratory background contributions, the memory effect in the sample introduction system and the concentration effect of double spike added, these factors have contributed to the large analytical uncertainty of ~8‰. As discussed above, Se (IV) suffers smaller cross contamination from Se(VI) than *vice versa*, leading to errors (±4.31‰ for Se(VI)) smaller than analytical errors of Se(IV) measurement. Therefore, only Se(VI) data was used to calculate the Se isotope exchange rate for ^{82}Se-enriched experiments. Based on initial $\delta^{82/76}Se(IV)$ and $\delta^{82/76}Se(VI)$, theoretical equilibrium fractionations and mass ratio of Se(IV) and Se(VI), the $\delta^{82/76}Se(IV)$ and $\delta^{82/76}Se(VI)$ at isotopic equilibrium should be 537.18‰, 537.65‰ and 538.35‰, and 550.96‰, 550.48‰ and 549.79‰ for EXP 8, 9, and 10, respectively. Using cross contamination-corrected $\delta^{82/76}Se(VI)$ data and Eqs. (2) and (3), the slopes of straight lines in the diagram for -Ln (1-F) vs. time can be obtained by linear regression analysis (Fig. 4). The exchange rate R derived from the best-fit line of EXP 10 is calculated to be 5.61×10^{-10} M day^{-1}. The upper bounds of possible exchange rates for EXP 8, 9 and 10 are estimated to be $\leq 6.34 \times 10^{-10}$ M day^{-1}, $\leq 1.12 \times 10^{-09}$ M day^{-1} and $\leq 1.17 \times 10^{-09}$ M day^{-1}, respectively (Table 4).

4.4. A possible isotope exchange mechanism

The extremely slow exchange kinetics between Se(IV) and Se(VI) suggest that electron transfers between these two species is not a straightforward process. Assuming only

Fig. 1. Se concentrations (left panels) and isotope compositions (right panels) for Se (IV) and Se (VI) under different experimental conditions: (A) 25 °C, 0.026 mM Se(IV) + 0.026 mM Se(VI); (B) 38 °C, 0.026 mM Se(IV) + 0.026 mM Se(VI); (C) 60 °C, 0.026 mM Se(IV) + 0.026 mM Se(VI); (D) 60 °C, 0.13 mM Se(IV) + 0.14 mM Se(VI); (E) 60 °C, 1.3 mM Se(IV) + 1.4 mM Se(VI). The red dotted lines in left panels represent the initial [Se(IV)]/[Se(VI)], and the dotted lines of red and blue in right panels represent the initial $\delta^{82/76}Se(VI)$ and $\delta^{82/76}Se(IV)$, respectively. (For interpretation of the references to colour in this figure legend, the reader is referred to the web version of this article.)
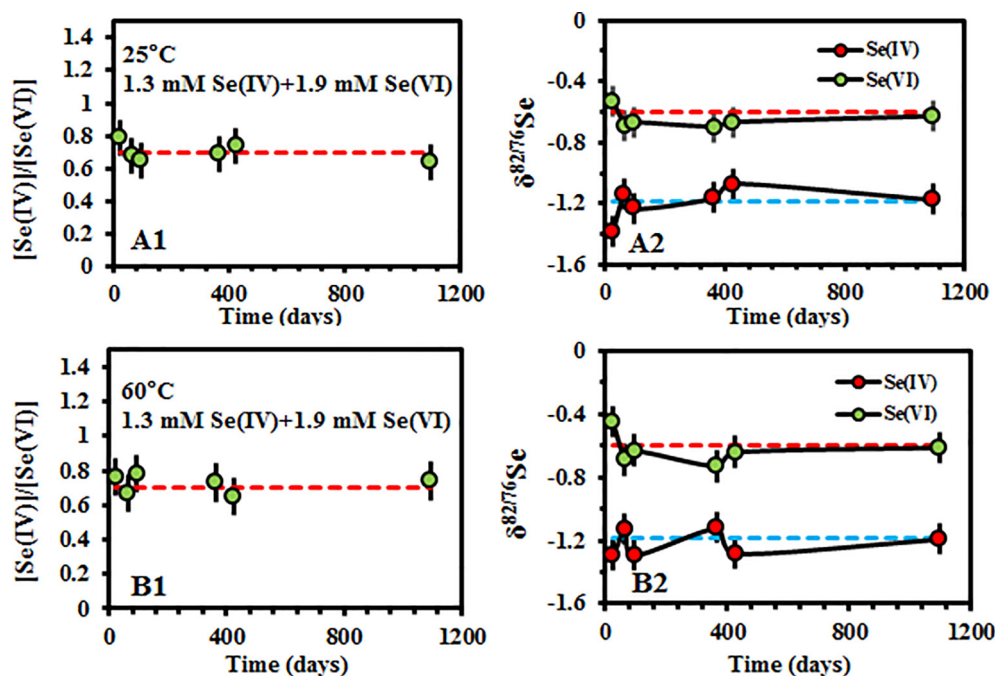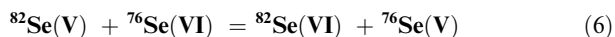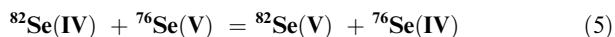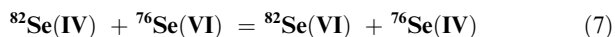
Fig. 2. Se concentrations (left panels) and isotope compositions (right panels) for Se (IV) and Se (VI) isotope exchange experiments, with 0.2 M AQDS added. (A) 25 °C; (B) 60 °C. The red dotted lines in A1 and B1 represent the initial [Se(IV)]/[Se(VI)], and the dotted lines of red and blue in A2 and B2 represent the initial $\delta^{82/76}Se(VI)$ and $\delta^{82/76}Se(IV)$, respectively. (For interpretation of the references to colour in this figure legend, the reader is referred to the web version of this article.)

one electron is transferred at a time, an intermediate transition state (Se(V)) such as $HSe_2O_7^{3-}$ (complexes of $HSeO_3^-$ and SeO_4^{2-}) must be formed (Rao and Badami, 1931; Sawyer and Humphreys, 1928; Ei-Absy et al., 1997). However, the concentration of Se(V) in solution is likely very low and unstable, which greatly reduces the probability of ion collisions, and thus electron transfers. In this process, a possible isotope exchange reaction sequence can be proposed:

$$^{82}Se(IV) + {}^{76}Se(VI) = {}^{82}Se(V) + {}^{76}Se(V) \qquad (4)$$
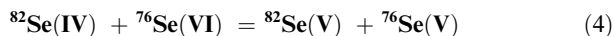
followed by subsequent reactions involving the two Se(V)'s,

$$^{82}Se(IV) + {}^{76}Se(V) = {}^{82}Se(V) + {}^{76}Se(IV) \qquad (5)$$

$$^{82}Se(V) + {}^{76}Se(VI) = {}^{82}Se(VI) + {}^{76}Se(V) \qquad (6)$$

with the overall exchange reaction being

$$^{82}Se(IV) + {}^{76}Se(VI) = {}^{82}Se(VI) + {}^{76}Se(IV) \qquad (7)$$

If two electrons are transferred simultaneously during one $^{82}Se(IV) + {}^{76}Se(VI)$ collision, the isotope exchange reaction can be described directly by equation (7). Whether one-electron or two-electron transfers during one Se(IV)–Se(VI) collision needs further investigation.

Transfer of electrons between Se(IV) and Se(VI) requires breaking of Se—O chemical bonds: Se(IV) is bound to three oxygen atoms in a pyramidal structure, whereas Se(VI) is bond to four oxygen atoms in a tetrahedral structure (Li and Liu, 2011). The Se—O bond length in Se(VI) (1.66–1.68 Å) is much shorter than that in Se(IV) (1.72–1.74 Å)

(Foster et al., 2003; Peak, 2006; Li and Liu, 2011), and thus breaking the Se—O bond in Se (VI) requires more energy. Therefore, we propose that breaking Se—O bonds in Se (VI) likely limits the isotope exchange between these two species. With the increase of pH, the bond breaking between the central ion and O becomes more and more difficult (Hall and Alexander, 1940). Simultaneously, due to the difference in chemical structures of $HSeO_3^-$ and SeO_4^{2-}, the configurations formed by the many nearby dipolar molecules around them are not the same. After electron transfer occurs, Se(IV) will be formed in a chemically unfavorable environment which was originally occupied by Se (VI), and so the energy barrier for reaction will be large (Marcus, 1993). In contrast, isotopic exchange between species with similar coordination environments is much faster. For example, both Fe (II) and Fe (III) are octahedrally coordinated, and they can reach isotopic equilibrium in a few minutes (Johnson et al., 2002; Welch et al., 2003). The extremely slow isotope exchange between Se(IV) and Se(VI) in this system is comparable to that between S(IV) and S(VI). At low temperatures, extremely slow isotope exchange kinetics was observed in the SO_3^{2-}-SO_4^{2-} system (Voge, 1939; Mcdonald, 1961; Fossing and Jørgensen, 1990; Fossing et al., 1992). Chiba and Sakai (1985) concluded that the sulfur atom at the center of the tetrahedral SO_4^- is strongly bound to four oxygen atoms, which hindered the isotope exchange between S(IV) and S(VI). Se (VI) has a similar tetrahedral structure as S(VI) (Peak, 2006; Fernandez-Martinez and Charlet, 2009; Li and Liu,
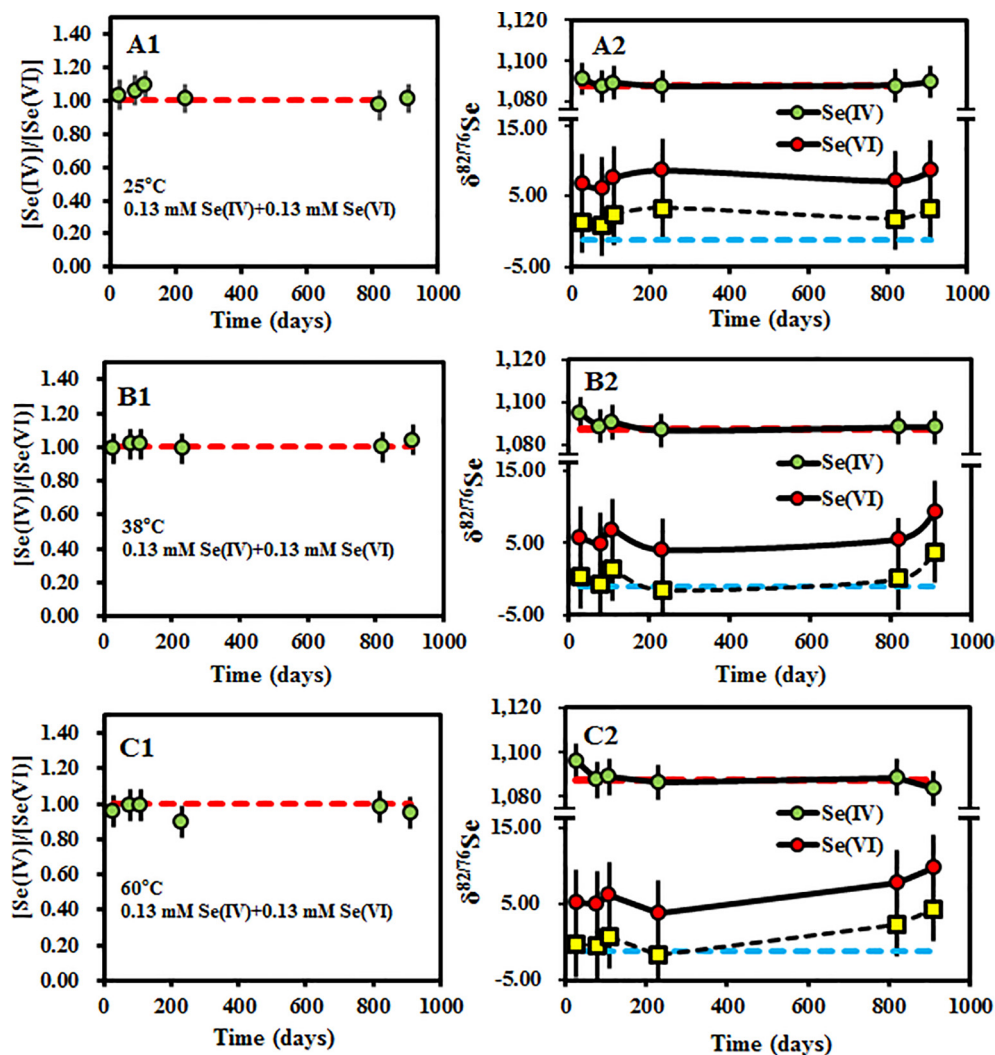
Fig. 3. Se concentrations (left panels) and isotope compositions (right panels) for Se (IV) and Se (VI) isotope exchange experiments, with Se (IV) doped with ^{82}Se. A, B and C represent experiments at 25 °C, 38 °C and 60 °C, respectively. The yellow symbols represent the $\delta^{82/76}$Se(VI) values corrected for cross contamination, the red dotted lines in left panels represent the initial [Se(IV)]/[Se(VI)], and the dotted lines of red and blue in right panels represent the initial $\delta^{82/76}$Se(VI) and $\delta^{82/76}$Se(IV), respectively. (For interpretation of the references to colour in this figure legend, the reader is referred to the web version of this article.)

2011), thus explaining the extremely slow exchange between Se(IV) and Se(VI).

4.5. pH effect on isotope exchange kinetics

The pH of most isotope exchange experiments in this study was 7. This pH is close to freshwater river and lake systems but is lower than typical ocean pH of ∼8 or higher than hydrothermal acidic pH. Our control experiment (without HEPES) was conducted at pH 3.5 and did not show detectable isotope exchange after 847 days (Fig. S3), suggesting that low pH does not facilitate isotope exchange between Se(IV) and Se(VI), at least over the experimental timescale. At higher pH, we expect the isotope exchange to be similar or slightly slower based on analogy to sulfur isotope exchange kinetics, where Hall and Alexander (1940) proposed that breaking of S—O bond in SO_4^{2-} is

more difficult at higher pH. However, to better understand pH effect on Se(IV)-Se(VI) isotope exchange more definitely, future experiments at low and high pH over even longer timescales are needed.

5. IMPLICATIONS

In recent years, the Se isotope system has been widely used to investigate the redox conditions in paleo-oceans and the geochemical cycles of Se in various settings (Johnson et al., 2000; Herbel et al., 2002; Clark and Johnson, 2010; Mitchell et al., 2012, 2016; Zhu et al., 2014; Wen et al., 2014; Stüeken et al., 2015a,b,c; Pogge von Strandmann et al., 2015; Kipp et al., 2017; Stüeken, 2017; König et al., 2019; Kurzawa et al., 2019). The pH value of the surface water environment is generally close to 7, thus allowing us to discuss the implications of our
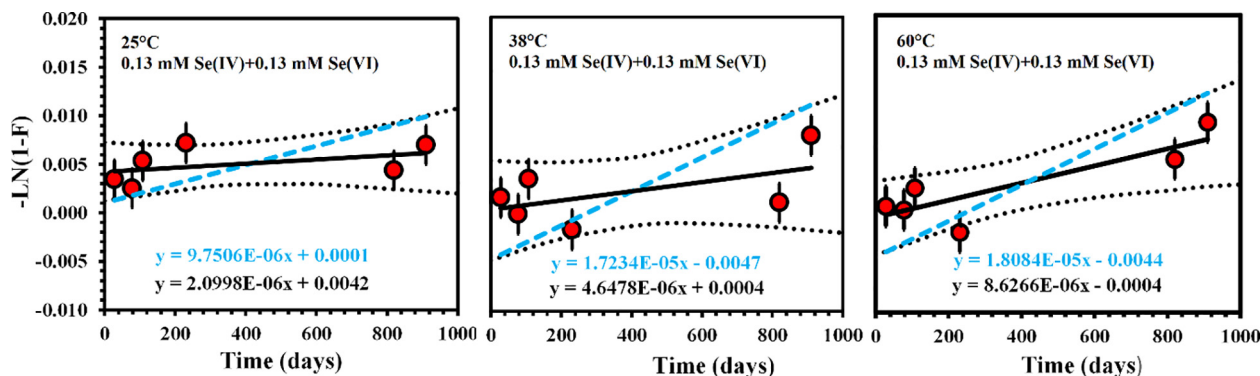
Fig. 4. Isotope exchange rates between aqueous Se(IV) and Se(VI) at 25 °C, 38 °C and 60 °C. The black solid lines are linear regressions (equation (3)) of experimental data. Isotope exchange rates are derived from the slopes of the regression lines. The black dashed curves refer to the 95% confidence interval of possible linear regression lines for EXP 8–10. The blue dashed lines represent the steepest lines (maximum slopes); the upper bounds of isotope exchange rates for EXP 8–10 are calculated using these maximum slopes. (For interpretation of the references to colour in this figure legend, the reader is referred to the web version of this article.)

experimental results in such settings. The maximum exchange rates for EXP 8–10 are estimated to be 6.34×10^{-10} M day^{-1}, 1.12×10^{-09} M day^{-1} and 1.17×10^{-09} M day^{-1}, respectively (Table 4 and Fig. 4). Application of these results from this study to natural conditions with much lower Se concentrations is difficult because we did not derive an empirical relationship between isotope exchange rates and Se concentrations due to extremely slow exchange rates. However, if we assume, provisionally, that the isotopic exchange rate obeys first order kinetics with respect to Se(IV) and Se(VI), as has been observed for the S(IV)-S(VI) system (Mcdonald, 1961):

$$R = \mathbf{k} \, [\mathbf{Se(IV)}] \, [\mathbf{Se(VI)}] \qquad (8)$$

isotope exchange rates in natural reservoirs can be extrapolated using Eq. (8). For example, the concentration and isotope composition of Se(IV) and Se(VI) in Colorado's Sweitzer Lake were determined to be 60.1 ± 20.2 nM (2SD, n = 13), 55.5 ± 31.1 nM (2SD, n = 13) and 2.83 ± 1.60‰ (2SD, n = 4), 3.13 ± 1.07‰ (2SD, n = 4), respectively (Clark and Johnson, 2010). An upper bound for the Se(IV) - Se(VI) isotope exchange rate in this lake can be estimated based on the results of EXP 8 because this experiment was conducted at 25 °C. We acknowledge that the slope in Fig. 4 for EXP 8 is not statistically significant, but the data clearly constrain the slope to be very small. Accordingly, we calculate a maximum exchange rate based on the upper bound of possible slope given the results of EXP 8. Assuming isotopic exchange follows first-order kinetics with respect to Se(IV) and Se(VI) (Eq. (8)), extrapolating the isotope exchange experimental results to Sweitzer Lake Se concentrations yields an exchange rate of $\leq 1.24 \times 10^{-16}$ M day^{-1} (Fig. 5R1), which translates to $t_{1/2}$ (calculated by setting F to 0.5 in Eq. (2)) and t_{min} (the minimum time for detectable isotope exchange in Se(IV) – Se(VI) systems, obtained by Eq. (9)) of 440,000 and 18,000 years, respectively.

$$t_{min} = -\mathrm{Ln}\left[1 - \frac{-0.2}{\delta_e(IV) - \delta_0(IV)}\right] / R \cdot \frac{[\mathrm{Se(IV)}][\mathrm{Se(VI)}]}{[\mathrm{Se(IV)}] + [\mathrm{Se(VI)}]} \qquad (9)$$

where 0.2 represents the minimum detectable change in $\delta^{82/76}$Se(IV) or $\delta^{82/76}$Se(VI). These timescales are much longer than the residence time of Se in Sweitzer Lake (2.4 years, Clark and Johnson, 2010). Therefore, isotope exchange between Se(IV) and Se(VI) is unlikely to have an effect on Se isotopic composition of Se(IV) and Se(VI). Sweitzer Lake has unusually high concentrations that have led to fish consumption restrictions. Accordingly, in most lakes, Se isotope shifts caused by isotopic exchange between aqueous Se(IV) and Se(VI) must be negligible.

In modern oceans, total dissolved inorganic Se (DISe) ranges from 0.6 to 1.6 nM (average 1 nM), and Se(IV)/Se(VI) ranges from 0.12 to 0.90 (average of 0.44; Measures and Burton, 1980; Measures et al., 1984; Cutter and Bruland, 1984; Aono et al., 1991; Cutter and Cutter, 1995, 1998, 2001). Thus, the concentration of Se(IV) and Se(VI) in seawater are ~6.9 nM and ~3.1 nM, respectively. Currently there are no species-dependent Se isotope data for seawater. Fortunately, the selection of initial δ values of Se (VI) and Se (VI) has little effect on determining the values of R, $t_{1/2}$ and t_{min}. Based on previously published deep seawater total Se isotope composition of 0.40 ± 0.05‰ (Chang et al., 2017) and an average Se(IV)/Se (VI) ratio of 0.44 (Measures and Burton, 1980; Measures et al., 1984; Cutter and Bruland, 1984; Aono et al., 1991; Cutter and Cutter, 1995, 1998, 2001; Chang, 2017), a simple mass balance constrains the relationship between seawater $\delta^{82/76}$Se(IV) and $\delta^{82/76}$Se(VI):

$$0.44 * \delta^{82/76}\mathrm{Se(IV)} + \delta^{82/76}\mathrm{Se(VI)} = 0.58 \qquad (10)$$

Assuming the difference between $\delta^{82/76}$Se(VI) and $\delta^{82/76}$Se(IV) is the same as that in Sweitzer Lake (0.30‰, n = 4) (Clark and Johnson, 2010), seawater $\delta^{82/76}$Se(IV) and $\delta^{82/76}$Se(VI) can be solved to be 0.19‰ and 0.49‰. Thus, according to the above calculated parameters, the R for seawater (Fig. 5R1) is extrapolated to be $\leq 7.96 \times 10^{-21}$ M day^{-1} from EXP 8 data, which translates to $t_{1/2}$ and t_{min} of ≥ 51 million and ≥ 3.6 million years, respectively. These timescales are much longer than the residence time of Se in modern oceans (<26,000 years; Large et al., 2015). Choosing drastically different $\delta^{82/76}$Se(IV)-
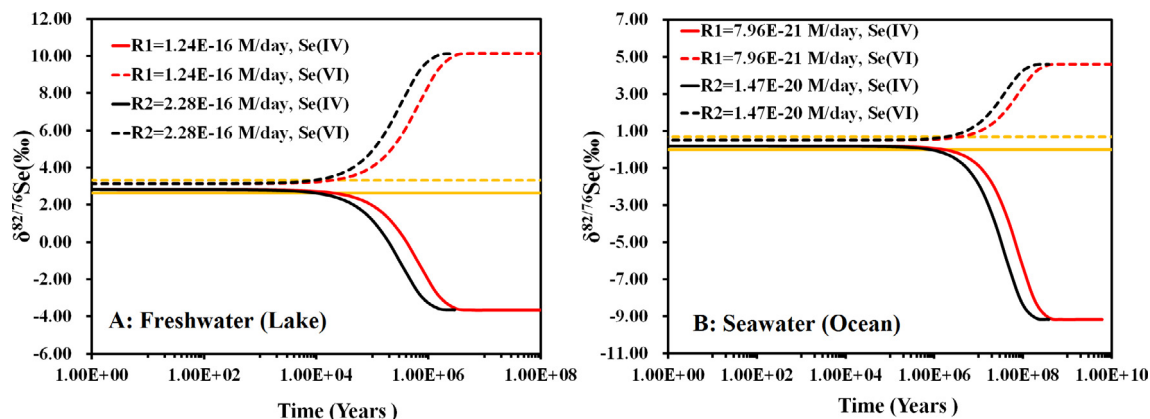
Fig. 5. Estimated timescales for isotope exchange in freshwater (A: lake) and seawater (B: Ocean). R1 and R2 are the upper bounds of exchange rates derived from EXP 8 and EXP 10, respectively. The yellow dashed and solid lines are the smallest values of $\delta^{82/76}$Se VI) and $\delta^{82/76}$Se (IV) distinguishable by MC-ICP-MS, respectively. (For interpretation of the references to colour in this figure legend, the reader is referred to the web version of this article.)

$\delta^{82/76}$Se(VI) offset from 0.00‰ to 0.81‰ (Maximum difference between $\delta^{82/76}$Se(VI) and $\delta^{82/76}$Se(VI) in Sweitzer Lake, Clark and Johnson, 2010) does not change this conclusion. Although the temperature of seawater was generally between 0 °C and 30 °C in geologic history, it was as high as 45 °C in some periods (such as late Cambrian) (Song et al., 2019). To explore the exchange rate in an extremely warm ocean, we apply the upper bound of the rate derived from the results of EXP 10 to estimate the lower limits of $t_{1/2}$ and t_{min} for isotope exchange between Se(IV) and Se(VI) in ocean; they are $\geq$27 million and $\geq$2 million years, respectively (Fig. 5). Therefore, isotope exchange is unlikely to matter in seawater as warm as 60 °C. Although organic ligands exist in seawater that can serve as electron shuttles, the results from EXP 6 and 7 indicate that any related increase in the exchange rate is not large enough to matter. On the early Earth, the level of free oxygen in the paleo-ocean or atmosphere was lower than it is now (Kump, 2008; Lyons et al., 2014). Hence, the residence time of Se should be lower than that of the present residence of 26,000 years (Stüeken et al., 2015b), making isotope exchange even less likely to matter.

6. CONCLUSIONS

Experiments designed to measure rates of isotopic exchange between Se(IV) and Se(VI) of natural isotopic compositions, at pH 7, concentrations up to 1.3 mM, and temperatures up to 60 °C revealed no detectable isotope fractionation within four years. Adding the electron shuttle AQDS did not increase the isotope exchange rate above the detection threshold.

In experiments that employed ^{82}Se-enriched Se(IV) to increase detection of very small amounts of exchange, there appears to be a slight systematic change in $\delta^{82/76}$Se(VI) after 910 days. Based on the results of three ^{82}Se-tracer experiments, we constrained the rate of isotope exchange to be $\leq 6.34 \times 10^{-10}$ M day^{-1} (25 °C; pH 7; 0.13 mM Se(IV) + 0.13 mM Se(VI)), $\leq 1.12 \times 10^{-09}$ M day^{-1} (38 °C; pH 7; 0.13 mM Se(IV) + 0.13 mM Se(VI)) and $\leq 1.17 \times 10^{-09}$ M day^{-1} (60 °C; pH 7; 0.13 mM Se(IV) + 0.13 mM Se(VI)).

Extrapolating these results to lower Se concentrations observed in a freshwater lake using an assumed first-order rate law, the time required to progress halfway to isotopic equilibrium ($t_{1/2}$) is estimated to be >440,000 years. The time required to shift the isotopic values by the minimum detectable amount (t_{min}) is >18,000 years. For the modern ocean, $t_{1/2}$ and t_{min} are estimated to be >51 million and >3.6 million years, respectively. These isotope exchange timescales are far longer than residence time in lakes and seawater. Therefore, the isotope changes between Se(IV) and Se(VI) in natural environment should be free from isotope exchange effects, and should be mainly controlled by reduction, adsorption and microbial assimilation or dissimilatory reduction.

Declaration of Competing Interest

The authors declare that they have no known competing financial interests or personal relationships that could have appeared to influence the work reported in this paper.

APPENDIX A. SUPPLEMENTARY MATERIAL

Supplementary data to this article can be found online at https://doi.org/10.1016/j.gca.2020.03.017.

REFERENCES

Aono T., Nakaguchi Y. and Hiraki K. (1991) Vertical profiles of dissolved selenium in the North Pacific. *Geochem. J.* **25**(1), 45–55.

Balistrieri L. S. and Chao T. T. (1990) Adsorption of selenium by amorphous iron oxyhydroxide and manganese dioxide. *Geochim. Cosmochim. Acta* **54**, 739–751.

Beard B. L., Handler R. M., Scherer M. M., Wu L., Czaja A. D., Heimann A. and Johnson C. M. (2010) Iron isotope fractionation between aqueous ferrous iron and goethite. *Earth Planet. Sci. Lett.* **295**(1–2), 241–250.

Brookins D. G. (1988) *Eh – pH Diagrams for Geochemistry*. Springer-Verlag, Berlin, pp. 18–19.

Cao X. and Bao H. (2017) Redefining the utility of the three-isotope method. *Geochim. Cosmochim. Acta* **212**, 16–32.

Catalano J. G., Zhang Z., Fenter P. and Bedzyk M. J. (2006) Inner-sphere adsorption geometry of Se(IV) at the hematite (100)-water interface. *J. Colloid Interface Sci.* **297**, 665–671.

Clark S. K. and Johnson T. M. (2010) Selenium stable isotope investigation into selenium biogeochemical cycling in a lacustrine environment: Sweitzer Lake, Colorado. *J. Environ. Qual.* **39**, 2200–2210.

Chang Y. (2017) Biogeochemical Processes of Dissolved Selenium and Isotopes in the Coastal Areas. Ph.D. thesis. East China Normal University, Shanghai, China.

Chang Y., Zhang J., Qu J. Q. and Xue Y. (2017) Precise selenium isotope measurement in seawater by carbon-containing hydride generation-Desolvation-MC-ICP-MS after thiol resin preconcentration. *Chem. Geol.* **471**(5), 65–73.

Chiba H. and Sakai H. (1985) Oxygen isotope exchange rate between dissolved sulfate and water at hydrothermal temperatures. *Geochim. Cosmochim. Acta* **49**, 993–1000.

Cutter G. A. (1982) Selenium in reducing waters. *Science* **217**(4562), 829–831.

Cutter G. A. and Bruland K. W. (1984) The marine biogeochemistry of selenium: A re-evaluation. *Limnol. Oceanogr.* **29**(6), 1179–1192.

Cutter G. A. and Cutter L. S. (1995) Behavior of dissolved antimony, arsenic, and selenium in the Atlantic Ocean. *Mar. Chem.* **49**(4), 295–306.

Cutter G. A. and Cutter L. S. (1998) Metalloids in the high latitude North Atlantic Ocean: Sources and internal cycling. *Mar. Chem.* **61**(1), 25–36.

Cutter G. A. and Cutter L. S. (2001) Sources and cycling of selenium in the western and equatorial Atlantic Ocean. *Deep-Sea Re. PT II: Top. Stud. Oceanogr.* **48**(13), 2917–2931.

Cutter G. A. and Cutter L. S. (2004) Selenium biogeochemistry in the San Francisco Bay estuary: changes in water column behavior. *Estuar. Coast. Shelf S.* **61**(3), 463–476.

Duc M., Lefèvre G. and Fédoroff M. (2006) Sorption of selenite ions on hematite. *J. Colloid Interface Sci.* **298**, 556–563.

Duc M., Lefèvre G., Fédoroff M., Jeanjean J., Rouchaud J. C., Monteil-Rivera F., Dumonceau J. and Milonjic S. (2003) Sorption of selenium anionic species on apatites and iron oxides from aqueous solutions. *J. Environ. Radioactiv.* **70**, 61–72.

Ei-Absy M. A., Ei-Enein M. A., Raieh M. and Aly H. F. (1997) Isotope exchange between 12-molybdocerate (IV) and sodium molybdate-^{99}Mo in aqueous media. *J. Radioanal. Nucl Chem.* **18**(2), 157–168.

Eldridge D. L., Guo W. and Farquhar J. (2016) Theoretical estimates of equilibrium sulfur isotope effects in aqueous sulfur systems: Highlighting the role of isomers in the sulfite and sulfoxylate systems. *Geochim. Cosmochim. Acta* **195**, 171–200.

Ellis A. S., Johnson T. M., Herbel M. J. and Bullen T. (2003) Stable isotope fractionation of selenium by natural microbial consortia. *Chem. Geol.* **195**, 119–129.

Fernández-Martínez A. and Charlet L. (2009) Selenium environmental cycling and bioavailability: a structural chemist point of view. *Rev. Environ. Sci. and Bio.* **8**(1), 81–110.

Fossing H. and Jørgensen B. B. (1990) Isotope exchange reactions with radiolabeled sulfur compounds in anoxic seawater. *Biogeochemistry* **9**(3), 223–245.

Fossing H., Thode-Andersen S. and Jørgensen B. B. (1992) Sulfur isotope exchange between ^{35}S-labeled inorganic sulfur compounds in anoxic marine sediments. *Mar. Chem.* **38**(1–2), 117–132.

Foster A. L., Brown G. E. and Parks G. A. (2003) X-ray absorption fine structure study of As (V) and Se (IV) sorption complexes on hydrous Mn oxides. *Geochim. Cosmochim. Acta* **67**, 1937–1953.

Frankanberger W. T. and Benson S. (1994) *Selenium in the Environment*. Marcel Dekker. Inc, New York, pp. 1–416.

Frierdich A. J., Beard B. L., Reddy T. R., Scherer M. M. and Johnson C. M. (2014a) Iron isotope fractionation between aqueous Fe (II) and goethite revisited: New insights based on a multi-direction approach to equilibrium and isotopic exchange rate modification. *Geochim. Cosmochim. Acta* **139**, 383–398.

Frierdich A. J., Beard B. L., Scherer M. M. and Johnson C. M. (2014b) Determination of the Fe (II) aq–magnetite equilibrium iron isotope fractionation factor using the three-isotope method and a multi-direction approach to equilibrium. *Earth Planet. Sci. Lett.* **391**, 77–86.

Gorski C. A., Handler R. M., Beard B. L., Pasakarnis T., Johnson C. M. and Scherer M. M. (2012) Fe atom exchange between aqueous Fe^{2+} and magnetite. *Environ. Sci. Technol.* **46**, 12399–12407.

Hall N. F. and Alexander O. R. (1940) Oxygen Exchange between Anions and Water. *J. Am. Chem. Soc.* **62**(12), 3455–3462.

Herbel M. J., Johnson T. M., Oremland R. S. and Bullen T. D. (2000) Fractionation of selenium isotopes during bacterial respiratory reduction of selenium oxyanions. *Geochim. Cosmochim. Acta* **64**(21), 3701–3709.

Herbel M. J., Johnson T. M., Tanji K. K., Gao S. and Bullen T. D. (2002) Selenium stable is agricultural drainage water management system. *J. Environ. Qual.* **31**, 1146–1156.

Hung J. and Shy C. (1995) Speciation of dissolved selenium in the Kaoping and Erhjen rivers and estuaries, southwestern Taiwan. *Estuaries* **18**(1), 234–240.

Igumnov S. A. (1976) Experimental study of sulfur isotope exchange between sulfide and sulfate sulfur in hydrothermal solution. *Geokhimiya* **4**, 497–503.

Johnson C. M., Skulan J. L., Beard B. L., Sun H., Nealson K. H. and Braterman P. S. (2002) Isotopic fractionation between Fe (III) and Fe (II) in aqueous solutions. *Earth Planet. Sci. Lett.* **195**, 141–153.

Johnson T. M. (2004) A review of mass-dependent fractionation of selenium isotopes and implications for other heavy stable isotopes. *Chem. Geol.* **204**, 201–214.

Johnson T. M. and Bullen T. D. (2003) Selenium isotope fractionation during reduction by Fe(II)-Fe(III) hydroxide-sulfate (green rust). *Geochim. Cosmochim. Acta* **67**(3), 413–419.

Johnson T. M., Bullen T. D. and Zawislanski P. T. (2000) Selenium stable isotope ratios as indicators of sources and cycling of selenium: Results from the northern reach of San Francisco Bay. *Environ. Sci. Technol.* **34**(11), 2075–2079.

Johnson T. M., Herbel M. J., Bullen T. D. and Zawislanski P. T. (1999) Selenium isotope ratios as indicators of selenium sources and oxyanion reduction. *Geochim. Cosmochim. Acta* **63**(18), 2775–2783.

Krouse H. R. and Thode H. G. (1962) Thermodynamic properties and geochemistry of isotopic compounds of selenium. *Can. J. Chem.* **40**, 367–375.

Kipp M. A., Stüeken E. E., Bekker A. and Buick R. (2017) Selenium isotopes record extensive marine suboxia during the Great Oxidation Event. *Proc. Natl. Acad. Sci. USA* **114**, 875–880.

König S., Eickmann B., Zack T., Yierpan A., Wille M., Taubald H. and Schoenberg R. (2019) Redox induced sulfur-selenium isotope decoupling recorded in pyrite. *Geochim. Cosmochim. Acta* **244**, 24–39.

Kump K. L. (2008) The rise of atmospheric oxygen. *Nature* **451**, 277–278.

Kurzawa T., König S., Alt J. C., Yierpan A. and Schoenberg R. (2019) The role of subduction recycling on the selenium isotope signature of the mantle: Constraints from Mariana arc lavas. *Chem. Geol.* **513**, 239–249.

Labidi J., König S., Kurzawa T., Yierpan A. and Schoenberg R. (2018) The selenium isotopic variations in chondrites are mass dependent; implications for sulfide formation in the early solar system. *Earth Planet. Sci. Lett.* **481**, 212–222.

Large R. R., Halpin J. A., Lounejeva E., Danyushevsky L. V., Maslennikov V. V., Gregory D., Sack P. J., Haines P. W., Long J. A., Makoundi C. and Stepanov A. S. (2015) Cycles of nutrient trace elements in the Phanerozoic Ocean. *Gondwana Res.* **28**, 1282–1293.

Layton-Matthews D., Leybourne M. I., Peter J. M., Scott S. D., Cousens B. and Eglington B. (2013) Multiple sources of selenium in ancient seafloor hydrothermal systems: compositional and Se, S, and Pb isotopic evidence from volcanic-hosted and volcanic-sediment-hosted massive sulfide deposits of the Finlayson Lake District, Yukon, Canada. *Geochim. Cosmochim. Acta* **117**, 313–331.

Li W., Beard B. L., Li C., Xu H. and Johnson C. M. (2015) Experimental calibration of Mg isotope fractionation between dolomite and aqueous solution and its geological implications. *Geochim. Cosmochim. Acta* **157**, 164–181.

Li W., Beard B. L. and Johnson C. M. (2011) Exchange and fractionation of Mg isotopes between epsomite and saturated MgSO4 solution. *Geochim. Cosmochim. Acta* **75**(7), 1814–1828.

Li X. and Liu Y. (2011) Equilibrium Se isotope fractionation parameters: A first-principles study. *Earth Planet. Sci. Lett.* **304**(1–2), 113–120.

Lyons T. W., Reinhard C. T. and Planavsky N. J. (2014) The rise of oxygen in Earth's early ocean and atmosphere. *Nature* **506**(7488), 307–315.

Macris C. A., Young E. D. and Manning C. E. (2013) Experimental determination of equilibrium magnesium isotope fractionation between spinel, forsterite, and magnesite from 600 to 800°C. *Geochim. Cosmochim. Acta* **118**, 18–32.

Marcus R. A. (1993) Electron transfer reactions in chemistry. Theory and experiment. *Rev. Mod. Phys.* **65**(3), 599–610.

Mcdonald R. L. (1961) *The kinetics of the sulfur (IV) - sulfur (VI) isotopic exchange reaction in aqueous and concentrated acid solutions. Ph.D. thesis.* Oregon State University, Corvallis, Oregon.

McKay H. (1938) Kinetics of exchange reactions. *Nature* **142**, 997–998.

McNeal J. M. and Balistrieri L. S. (1989) Geochemistry and occurrence of selenium; an overview. In: Selenium in Agriculture and the Environment. SSSA Special Publication. (ed. L. W. Jacobs). Soil Science Society of America, Madison, WI, pp. 1–13.

Measures C. and Burton J. (1980) The vertical distribution and oxidation states of dissolved selenium in the northeast Atlantic Ocean and their relationship to biological processes. *Earth Planet. Sci. Lett.* **46**(3), 385–396.

Measures C., Grant B., Khadem M., Lee D. S. and Edmond J. M. (1984) Distribution of Be, Al, Se and Bi in the surface waters of the western North Atlantic and Caribbean. *Earth Planet. Sci. Lett.* **71**(1), 1–12.

Mitchell K., Couture R. M., Johnson T. M., Mason P. R. D. and Cappellen P. V. (2013) Selenium sorption and isotope fractionation: Iron (III) oxides versus iron (II) sulfides. *Chem. Geol.* **342**, 21–28.

Mitchell K., Mansoor S. Z., Mason P. R. D., Johnson T. M. and Van Cappellen P. (2016) Geological evolution of the marine selenium cycle: Insights from the bulk shale $\delta^{82/76}$Se record and isotope mass balance modeling. *Earth Planet. Sci. Lett.* **441**, 178–187.

Mitchell K., Mason P. R. D., Cappellen P. V., Johnson T. M., Twill B. C., Owens J. D., Diaz J., Ingall E. D., Reichart G. J. and Lyons T. W. (2012) Selenium as paleo-oceanographic proxy: a first assessment. *Geochim. Cosmochim. Acta* **89**, 302–317.

Nurmi J. T. and Tratnyek P. G. (2002) Electrochemical properties of natural organic matter (NOM), fractions of NOM, and model biogeochemical electron shuttles. *Environ. Sci. Technol.* **36**, 617–624.

Oremland R. S., Hollibaugh J. T., Maest A. S., Presser T. S., Miller L. G. and Culbertson C. W. (1989) Selenate reduction to elemental selenium by anaerobic bacteria in sediments and culture: biogeochemical significance of a novel, sulfate-independent respiration. *Appl. Environ. Microb.* **55**(9), 2333–2343.

Peak D. (2006) Adsorption mechanisms of selenium oxyanions at the aluminum oxide/water interface. *J. Colloid Interf. Sci.* **303**(3), 337–345.

Pezzarossa B., Piccotino D. and Petruzzelli G. (1999) Sorption and desorption of selenium in different soils of the mediterranean area. *Commun. Soil Sci. Plant Anal.* **30**(19–20), 2669–2679.

Pogge von Strandmann P. A. E., Stüeken E. E., Elliott T., Poulton S., Dehler C. M., Canfield D. E. and Catling D. C. (2015) Selenium isotope evidence for progressive oxidation of the Neoproterozoic biosphere. *Nat. Commun.* **6**, 1–10.

Qin H. B., Takeichi Y., Nitani H., Terada Y. and Takahashi Y. (2017a) Tellurium distribution and speciation in contaminated soils from abandoned mine tailings: comparison with selenium. *Environ. Sci. Technol.* **51**(11), 6027–6035.

Qin H. B., Zhu J. M., Lin Z. Q., Xu W. P., Tan D. C., Zheng L. R. and Takahashi Y. (2017b) Selenium speciation in seleniferous agricultural soils under different cropping systems using sequential extraction and X-ray absorption spectroscopy. *Environ. Pollut.* **225**, 361–369.

Rao K. R. and Badami J. S. (1931) Investigations on the Spectrum of Selenium. Part I. Se IV and Se V. *P. Roy. Soc. A-Math. Phy.* **131**(131), 154–169.

Reddy T. R., Frierdich A. J., Beard B. L. and Johnson C. M. (2015) The effect of pH on stable iron isotope exchange and fractionation between aqueous Fe (II) and goethite. *Chem. Geol.* **397**, 118–127.

Rees C. E. and Thode H. G. (1966) Selenium isotope effects in the reduction of sodium selenite and of sodium selenate. *Can. J. Chem.* **44**, 419–427.

Robberecht H. and Grieken R. V. (1982) Selenium in environmental waters: Determination, speciation and concentration levels. *Talanta* **29**(10), 823–844.

Rouxel O., Fouquet Y. and Ludden J. N. (2004) Subsurface processes at the lucky strike hydrothermal field, mid-atlantic ridge: evidence from sulfur, selenium, and iron isotopes. *Geochim. Cosmochim. Acta* **68**(10), 2295–2311.

Rouxel O., Ludden J., Carignan J., Marin L. and Fouquet Y. (2002) Natural variations of Se isotopic composition determined by hydride generation multiple collector inductively coupled plasma mass spectrometry. *Geochim. Cosmochim. Acta* **66**, 3191–3199.

Rovira M., Gimenez J., Martinez M., Martinez-Llado X., de Pablo J., Marti V. and Duro L. (2008) Sorption of selenium (IV) and selenium (VI) onto natural iron oxides: goethite and hematite. *J. Hazard. Mater.* **150**, 279–284.

Sakai H. (1983) Sulfur isotope exchange rate between sulfate and sulfide and its application. *Geothermics* **12**(2–3), 111–117.

Sakai H. and Dickson F. W. (1978) Experimental determination of the rate and equilibrium fractionation factors of sulfur isotope exchange between sulfate and sulfide in slightly acid solutions at 300°C and 1000 bars. *Earth Planet. Sci. Lett.* **39**(1), 151–161.

Saeki K. and Matsumoto S. (1994) Selenite adsorption by a variety of oxides. *Commun. Soil Sci. Plan.* **25**(11–12), 2147–2158.

Saeki K., Matsumoto S. and Tatsukawa R. (1995) Selenite adsorption by manganese oxides. *Soil Sci.* **160**, 265–272.

Sawyer R. A. and Humphreys C. J. (1928) Electron-system spectra of arsenic and selenium. *Phys. Rev.* **32**(4), 583–592.

Schauble E. A. (2004) Applying stable isotope fractionation theory to new systems. *Rev. Mineral. Geochem.* **55**, 65–111.

Schilling K., Johnson T. M., Dhillon K. S. and Mason P. R. D. (2015) Fate of selenium in soils at a seleniferous site recorded by high precision Se isotope measurements. *Environ. Sci. Technol.* **49**(16), 9690–9698.

Schilling K., Johnson T. M. and Wilcke W. (2011) Isotope fractionation of selenium during fungal biomethylation by Alternaria alternate. *Environ. Sci. Technol.* **45**(7), 2670–2676.

Schilling K., Johnson T. M. and Wilcke W. (2013) Isotope fractionation of selenium by biomethylation in microcosm incubations of soil. *Chem. Geol.* **352**, 101–107.

Shahar A., Young E. D. and Manning C. E. (2008) Equilibrium high-temperature Fe isotope fractionation between fayalite and magnetite: an experimental calibration. *Earth Planet. Sci. Lett.* **268**(3–4), 330–338.

Shaker A. M. (1996) Kinetics of the reduction of Se (IV) to Se-Sol. *J. Colloid Interf. Sci.* **180**(1), 225–231.

Skulan J. L., Beard B. L. and Johnson C. M. (2002) Kinetic and equilibrium Fe isotope fractionation between aqueous Fe(III) and hematite. *Geochim. Cosmochim. Acta* **66**, 2995–3015.

Song H., Wignall P. B., Song H., Dai X. and Chu D. (2019) Seawater temperature and dissolved oxygen over the past 500 million years. *J. Earth Sci.* **30**, 236–243.

Stüeken E. E., Buick R. and Anbar A. D. (2015a) Selenium isotopes support free O$_2$ in the latest Archean. *Geology* **43**, 259–262.

Stüeken E. E., Buick R., Bekker A., Catling D. C., Foriel J., Guy B. M., Kah L. C., Machel H. G., Montanez I. P. and Poulton S. W. (2015b) The evolution of the global selenium cycle: Secular trends in Se isotopes and abundances. *Geochim. Cosmochim. Acta* **162**, 109–125.

Stüeken E. E., Foriel J., Buick R. and Schoepfer S. D. (2015c) Selenium isotope ratios, redox changes and biological productivity across the end-Permian mass extinction. *Chem. Geol.* **410**, 28–39.

Stüeken E. E. (2017) Selenium isotopes as a biogeochemical proxy in deep time. *Rev. Mineral. Geochem.* **82**, 657–682.

Varas-Reus M. I., König S., Yierpan A., Lorand J. P. and Schoenberg R. (2019) Selenium isotopes as tracers of a late volatile contribution to Earth from the outer Solar System. *Nat. Geosci.* **12**, 779–782.

Voge H. H. (1939) Exchange reactions with radiosulfur. *J. Am. Chem. Soc.* **61**(5), 1032–1035.

Wang X. L., Johnson T. M. and Ellis A. S. (2015a) Equilibrium isotopic fractionation and isotopic exchange kinetics between Cr(III) and Cr(VI). *Geochim. Cosmochim. Acta* **153**, 72–90.

Wang X. L., Johnson T. M. and Lundstrom C. C. (2015b) Low temperature equilibrium isotope fractionation and isotope exchange kinetics between U(IV) and U(VI). *Geochim. Cosmochim. Acta* **158**, 262–275.

Welch S. A., Beard B. L., Johnson C. M. and Braterman P. S. (2003) Kinetic and equilibrium Fe isotope fractionation between aqueous Fe(II) and Fe(III). *Geochim. Cosmochim. Acta* **67**, 4231–4250.

Wen H., Carignan J., Chu X., Fan H., Cloquet C., Huang J., Zhang Y. and Chang H. (2014) Selenium isotopes trace anoxic and ferruginous seawater conditions in the Early Cambrian. *Chem. Geol.* **390**, 164–172.

Wiesli R. A., Beard B. L. and Johnson C. M. (2004) Experimental determination of Fe isotope fractionation between aqueous Fe (II), siderite and "green rust" in abiotic systems. *Chem. Geol.* **211**, 343–362.

Wu L., Beard B. L., Roden E. E. and Johnson C. M. (2011) Stable iron isotope fractionation between aqueous Fe(II) and hydrous ferric oxide. *Environ. Sci. Technol.* **45**, 1847–1852.

Wu L., Beard B. L., Roden E. E., Kennedy C. B. and Johnson C. M. (2010) Stable Fe isotope fractionations produced by aqueous Fe(II)-hematite surface interactions. *Geochim. Cosmochim. Acta* **74**, 4249–4265.

Xu W., Zhu J. M., Johnson T. M., Wang X., Lin Z. Q., Tan D. and Qin H. (2020) Selenium isotope fractionation during adsorption by Fe, Mn and Al oxides. *Geochim. Cosmochim. Acta* **272**, 121–136.

Yao Q. Z. and Zhang J. (2005) The behavior of dissolved inorganic selenium in the Bohai Sea. *Estuar. Coast. Shelf S.* **63**(1), 333–347.

Yierpan A., König S., Labidi J. and Schoenberg R. (2019) Selenium isotope and S-Se-Te elemental systematics along the Pacific-Antarctic ridge Role of mantle processes. *Geochim. Cosmochim. Acta* **249**, 199–224.

Yierpan A., König S., Labidi J., Kurzawa T., Babechuk M. G. and Schoenberg R. (2018) Chemical sample processing for combined selenium isotope and selenium–tellurium elemental investigation of the earth's igneous reservoirs. *Geochem. Geophy. Geosy.* **19**(2), 516–533.

Zink S., Schoenberg R. and Staubwasser M. (2010) Isotopic fractionation and reaction kinetics between Cr(III) and Cr(VI) in aqueous media. *Geochim. Cosmochim. Acta* **74**(20), 5729–5745.

Zhang P. and Sparks D. L. (1990) Kinetics of Selenate and Selenite Adsorption Desorption at the Goethite Water Interface. *Environ. Sci. Technol.* **24**, 1848–1856.

Zhu J. M., Johnson T. M., Clark S. K., Zhu X. K. and Wang X. L. (2014) Selenium redox cycling during weathering of Se-rich shales: A selenium isotope study. *Geochim. Cosmochim. Acta* **126**, 228–249.

Zhu J. M., Johnson T. M., Finkelman R. B., Zheng B., Sýkorová I. and Pešek J. (2012) The occurrence and origin of selenium minerals in Se-rich stone coals, spoils and their adjacent soils in Yutangba, China. *Chem. Geol.* **330–331**, 27–38.

Zhu J. M., Johnson T. M., Clark S. K. and Zhu X. K. (2008) High precision measurement of selenium isotopic composition by hydride generation multiple collector inductively coupled plasma mass spectrometry with a ^{74}Se-^{77}Se double spike. *Chinese J. Anal. Chem.* **36**(10), 1385–1390.

Zhu J. M., Zuo W., Liang X. B., Li S. H. and Zheng B. S. (2004) Occurrence of native selenium in Yutangba and its environmental implications. *Appl. Geochem.* **19**, 461–467.

Associate editor: Stefan Weyer